BIOLOGIJA. 2008. Vol. 54. No. 4. P. 283–289
DOI: 10.2478/v10054-008-0058-9

Improved proteomic characterization of human myocardium and heart conduction system by computational methods

Dalius Matuzevičius[1],

Edvardas Žurauskas[2],

Rūta Navakauskienė[3, 4*],

Dalius Navakauskas[1]

[1] *Department of Electronic Systems, Faculty of Electronics, Vilnius Gediminas Technical University, Naugarduko 41-422, LT-03227 Vilnius, Lithuania*

[2] *Faculty of Medicine, Vilnius University, M. K. Čiurlionio 21, LT-03101 Vilnius, Lithuania*

[3] *Department of Developmental Biology, Institute of Biochemistry, Mokslininkų 12, LT-08662 Vilnius, Lithuania*

[4] *Department of Chemistry and Bioengineering, Faculty of Fundamental Sciences, Vilnius Gediminas Technical University, Saulėtekio al. 11, LT-10223 Vilnius, Lithuania*

Cardiovascular diseases are among the leading causes of mortality in the developing countries. The cardiac conduction system consists of distinctive heart muscle cells that initiate and propagate the electric impulse required for coordinated contraction. This myogenic system performs a distinguished function and has features not characteristic of the ordinary myocardium. Disturbances of the conduction system may cause life-threatening heart beat disorders. The proteomic analysis of the human conduction system is still limited. In the present study, we have employed computational methods to characterize proteins of the human myocardium and heart the conduction system. We present the computational methods that empowered us to assess the changes in protein expression level as well as to characterize them by exact molecular weight and pI. The changes in protein expression level in human myocardium and heart conduction system reveal the necessity to identify these proteins especially specific of the heart conduction system.

Key words: human myocardium, MC, heart conduction system, HCS, 2-DE fractionation, heart tissue proteomic analysis, computational methods

INTRODUCTION

Cardiovascular diseases are among the leading causes of morbidity and mortality in Western societies and developing countries. The ability to investigate the complete proteome provides a critical tool toward elucidating the complex and multifactorial basis of cardiovascular biology, especially disease processes. In recent years, the proteome of the most relevant cellular elements of the cardiovascular system has begun to be depicted with the construction of two-dimensional gel electrophoresis maps and databases [1]. One of the most important elements of the heart is the conduction system. The conduction system of the heart comprises the sinoatrial node, atrioventricular node, and the His bundle which ramifies to the left and right branches and ends in the subendocardium of the corresponding ventricles. The conduction system is the means by which heart beat is initiated and propagated quickly into the different parts of the myocardium in a regular, orderly fashion resulting in the most effective heart contraction. This myogenic system plays a distinguished function and has features not characteristic of the ordinary myocardium. The heart conduction system has a faster transmission of the bioelectrical impulse than the myocardium and is responsible for depolarization (heartbeat) control. Disturbances of the conduction system may cause life-threatening heart beat

* Corresponding author. E-mail: ruta.navakauskiene@bchi.lt.

disorders. The precise molecular mechanism of the combined conductive performance of the heart conduction system cells has not yet been identified. The first attempt to investigate the protein composition of the conduction system has been performed only recently, and one protein group (around 26 kDa) has been found specific for the conduction system [2].

Proteomic approaches might help to close the gap between traditional pathophysiologic and more recent genomic studies, assisting our basic understanding of cardiovascular diseases [3, 4]. The application of proteomics in cardiovascular medicine gives great promise. The analysis of heart tissue and plasma / serum specimens has the potential to provide unique information on the patient and on the human proteome in general. Currently available clinical applications of proteomics are limited and focus mainly on cardiovascular biomarkers of chronic heart failure and myocardial ischemia [5].

The main goal of the present study was to characterize the total proteins isolated from human heart tissues – myocardium and heart conduction system, and fractionated in 2DE by computational methods. For the analysis, we used the protein fractionation technology in the 2DE system, and protein maps were analysed by computational methods. More extensive proteomic studies are required to identify the proteins that are specific in the distinct human heart tissues by mass spectrometry methods. Human heart proteomics may have promising applications in clinical medicine.

MATERIALS AND METHODS

Tissue disruption

The conduction system was examined in human heart autopsy specimens. Heart preparations of adult humans were chosen randomly, irrespective of age, sex or pathology.

The fact that the conduction system of the heart is surrounded by the connective tissue allowed us to separate it from the ordinary myocardium. Conduction system tissue is more transparent and brighter than myocardium tissue and can be recognized microscopically even utilizing middle magnification (12–36 times).

In our specimens, the artery of the atrioventricular (AV) node branched from the right coronary artery on the same level as the posterior interventricular sulcus. It was separated up to the middle level of the septal tricuspid leaflet close to the front of the coronary sinus. On this level, the artery penetrates the back pole of the AV node or gets into the posterior part of the interventricular septum under the node. To find the anterior pole of the AV node, a connection between the central fibrous body and the fibrous ring of the tricuspid valve had to be disclosed. To this end, endocardium, soft tissues and myocardium had to be separated from the central fibrous body. Going down, a connection between the right slope of the central fibrous body and the tricuspid ring was found. It corresponds to the level of the anterior commissura of tricuspid valve. Then the basement of the fibrous ring of the septal tricuspid leaflet was separated from the soft tissues up to the back node pole, thus finishing the artery preparation. In this way, the right edge of the node was discovered. The preparation was eased by the fact that the connective tissue coating the AV node is joined to the tricuspid fibrous ring. This allowed a precise separation of the right edge of the node. To find the left edge of the node, the soft tissues covering the AV node were separated 4–6 mm in width (it corresponds to the node width). So the whole AV node was disclosed completely together with the atrial part of the His bundle (HB) located close to the junction of the right tricuspid fibrous ring with the central fibrous body or 1–1.5 mm behind it. The penetrating part of the bundle can be easily found after breaking the junction between the central fibrous body and the fibrous ring of the tricuspid valve. The following steps were performed: a branch of the scissors was introduced under the right edge of the central fibrous body close to the junction with the tricuspid fibrous ring, and the junction was cut. The bifurcation of the HB is located on the border between the membranous part of the interventricular septum and the crest of the muscular interventricular septum part. Firstly, the top right borders of the HB ventricular part were separated from the surrounding tissues, and then the left edge (with the very thin left branch) was found. There were no difficulties in disclosing the HB branches by their fixed location.

The samples of the conduction system tissues used for the 2DE studies were abstracted from the His bundle. Specimens of tissues prepared from hearts (conduction system, ordinary myocardium and mitral valve) were fixed in liquid nitrogen.

Total protein isolation from heart tissue

Fresh tissue dissected from human myocardium and heart conduction system was rinsed briefly with ice-cold buffer (PBS) and blot dry. A tissue sample was pulverized in liquid nitrogen with a pestle until it was a uniform powder. To the pulverized tissue, an appropriate volume of the Chemicon Total Protein Extraction Kit reagent was added and the tissue cell lysate was transferred to the tube, and further the heart total proteins were isolated according to the manufacturer's protocol (Chemicon International, Inc.). The total tissue proteins were examined immediately or stored at –70 °C.

Protein fractionation in 2DE system

The total tissue proteins were resolved by two-dimensional gel electrophoresis (2DE). An Immobiline DryStrip Kit, pH range 3–10, and Excel Gel SDS, gradient 8–18% were used for 2DE. It was carried out according to the manufacturer's instructions (Immobiline DryStrip Kit for 2-D Electrophoresis with Immobiline DryStrip and ExelGel SDS, Amersham Pharmacia, Uppsala, Sweden). For analysis of total hart tissue proteins, 2DE gels were stained using the PageBlue Protein Staining Solution (PageBlue Protein Staining Protocol, Fermentas, Lithuania).

Computational analysis

For a fast, accurate and easy analysis of two-dimensional electrophoresis, gel specialized software [6, 7] or even systems [8] can be used. Dedicated software enables to track changes of protein spots, quantify and display them on-screen, save or export data and make spot analysis more reliable. The spot matching and data basing tools make it possible to quickly and objectively compare hundreds of different gels. In this research, the prototype of a new software tool for 2DE gel image analysis was used. The prototype is implemented in Matlab environment and has

built-in original image processing algorithms composed using new, advanced and powerful image processing methods.

Once a gel has been scanned, a standard computer-assisted analysis of 2DE gels includes at least the following three basic steps [9]:

1) pre-processing of images;

2) detection and quantification of a protein spot;

3) alignment of images (gel-to-gel matching of spot patterns) and differential analysis.

In the following sections, we comment on the main computational analysis procedures.

Image digitization and preprocessing

Digitization of gels was performed using UMAX tools – PowerLook III scanner together with MagicScan 4.6 software. Two-dimensional electrophoresis gels are scanned at 300 dpi resolution and saved in TIFF format files. Then the digitized images are loaded into the software tool. Before the automatic image alignment and analysis, images need to be pre-processed (registered).

The first step of the image pre-processing stage is to reject unnecessary and erroneous parts of the image, primarily edges of image that are free from protein spots. It reduces the computational load, lowers the probability of erroneous detections and improves the quality of the input images prior to segmentation. In the image under investigation, the user interactively marks two areas (see Fig. 1) – the protein map analysis area (marked by red and blue rectangles) and the working area (which additionally includes MW markers). **Removal of 2DE gel edges** is done with a developed software tool.

The second step of the pre-processing stage is **image filtering**. Two pre-processed images – one for the protein segmentation and the other for protein parameter estimation purposes – are computed (let us call them I_S and I_E, respectively). During this computational step, three distinct operations with the images are performed: *initial background subtraction*, *image smoothing* and *false spots suppression*. The use of all three operations yields the pre-processed image I_S, while the use of the first two operations with specific parameters (presented later) yields the pre-processed image I_E. Let us briefly comment on each operation.

Initial background subtraction is applied to eliminate meaningless changes in the gel background intensity level. The gradually changing background is detected by the morphological approach. We use the Top-Hat operation – morphologically opened image g_{ij}^{open} subtraction from the original image G_{ij}. The employed structuring element H_{ij} is a disk with a radius of 70 px. The whole Top-Hat operation can be expressed as

$$\widehat{g}_{ij} = G_{ij} - g_{ij}^{\text{open}} = G_{ij} - ((g_{ij} \ominus H_{ij}) \oplus H_{ij}),$$

here g_{ij}^{open} morphological opening is explicitly expressed by the use of morphological operations: dilation $g_{ij}^{\max} = G_{ij} \oplus H_{ij}$ $g_{ij}^{\min} = G_{ij} \ominus H_{ij}$ and erosion.

Image smoothing is needed to remove the impulse noise that corrupts the images. Impulse noise appears during image acquisition when the scanning devices pick up dust particles. This type of noise can be effectively reduced by smoothing images with a local median filter [10] which removes small noise features on the image while leaving larger features like spots unaffected:

$$g_{\text{ij}}^{\text{med}} = \text{median}\left[\text{sort}\left(g_{i+\Delta^i, j+\Delta^j}\right)\right],$$

here g_{ij} is a pixel value; $\Delta^i \in (-k, -k+1, \ldots, k)$; $\Delta^j \in (-k, -k+1, \ldots, k)$; $k = (K-1)/2$. The employed median filter has the window size $K = 9$ px for the I_S image and $K = 3$ px for the I_E image.

False spots suppression is a necessary operation which reduces the segmentation error considerably. It is performed by: a) the search for local intensity minima, b) a simple check of their depth $h \le 5$ (for image pixel values in [0.255] range); c) check of their basement area $s \le 10$ px ; and d) local image intensity correction if both queries are true.

Protein spot detection and quantification

In order to detect protein spots, **image segmentation** is preformed. The pre-processed 2DE images I_S are segmented into regions with the use of a semi-automated algorithm employing *Watershed transform*. Local minima are the most probable candidates for protein spot centers and thus justify the use of Watershed transform which segments the image into regions with a single minimum [11]. However, since automatic false spot suppression does not guarantee removal of all false spots, usually over-segmentation after Watershed transform application occurs. The developed software tool enables the user to correct (split or merge) segmentation results interactively. Afterwards results (contours and spot intensities) of semi-automated image segmentation are automatically adjusted using of a less distorted image I_E.

Protein spot parameterization needs to be done in order to quantify individual protein spots. Thus, each segmented 2DE image region containing a spot is modeled fitting a parametric model. A parametric protein spot model is a functional description of an idealized spot shape with parameters that have to be optimized. The parametric spot model used is a *bell-shaped two-dimensional function*:

$$S_{BF}(i, j) = \frac{1}{1 + \left(\frac{i - c_i}{a_i}\right)^{2b_i}} \cdot \frac{1}{1 + \left(\frac{j - c_i}{a_j}\right)^{2b_j}},$$

here a is a slope distance to the spot centre; b is a slope steepness; c is the centre of the shape. Other mathematical spot models [12] can be used, but it was shown [13] that the Bell-shaped model is better to handle saturated spots.

After protein spot shape modeling, spot centre coordinates (c_j, c_j) are recorded and spot quantity calculation is approached. Spot quantity V is defined as the total intensity of a spot in a gel image and corresponds to the amount of protein in the actual spot on the gel. The total intensity of an object is the sum of the intensities of all the pixels that make up the object:

$$V = \sum_{(i,j) \in \text{spot}} G(i, j).$$

The quantity of each protein spot in a gel V is divided by the total quantity of all the protein spots in that gel V_Σ in

order to obtain the final normalized quantity V of the given spot:

$$V = \frac{V}{V_{\Sigma}} \cdot$$

The process of normalization compensates for no expression-related variations in spot intensity and provides for an accurate comparison of spot quantities among the gels done in the following stage.

Image alignment and differential analysis

In order to compare protein spots from different 2DE gel images, protein spots need to be matched [14]. **The matching procedure** usually requires to define the landmarks that are common to both images. Thus, landmarks are reference points used to align and warp gel images. Almost all landmarks are calculated automatically by our original algorithm which uses a combination of calculations of cross-correlation through the Fourier transform and mutual information. Moreover, image warping is done iteratively, starting from major landmarks and in each iteration computing *Thin-Plate Spline Transformation* [15] of a warped image.

After pairing the protein spots in gel images, a ratio of spots normalized quantities among the images is calculated:

$$\hat{r}_{1/2} = \frac{\hat{V}_{G1}}{\hat{V}_{G2}} \text{ and } \hat{r}_{2/1} = \frac{\hat{V}_{G2}}{\hat{V}_{G1}},$$

here $\hat{V}_{G1}$ is a normalized quantity of the first gel; and $\hat{V}_{G2}$ is a normalized quantity of the second gel. One can notice that $\hat{r}_{1/2} > 1$ when the spot from the second gel is smaller and $\hat{r}_{2/1} > 1$ when the spot from the second gel is larger.

The protein spot normalized quantity ratio is used to determine whether a spot in the first image was larger than the corresponding spot in the second image, or vice versa. The computed values for protein spots under investigation are shown in Table.

RESULTS AND DISCUSSION

Two-dimensional electrophoretic patterns of total proteins in heart tissues

Proteomic analysis of heart tissue is complicated by the large dynamic range of its proteins. In our studies, we have isolated total proteins from two human heart parts – the myocardium and the heart conduction system – and proteins were fractionated by two-dimensional electrophoresis – one of the main technologies of proteomics. Importantly, this technology allows analysis of a large spectrum of proteins and in our study was performed in the pH range 3–10 IEF strips and SDS / PAGE gradient.

As one can see in Fig. 1, up to 200 polypeptides were detected by Coomassie staining in human myocardium tissue (Fig. 1A). The number of total polypeptides in the human myocardium (Fig. 1A) was much higher than in the human heart conduction system (Fig. 1B). We have found that proteins nos. 1, 2, 3 and 4 (Figs. 1–3, Table) are much more pronounced in the human myocardium tissue than in the human heart conduction system. Only the expression of protein no. 5 was lower in the heart conduction system.

Changes in protein expression level in human myocardium and heart conduction system reveal the necessity to identify these proteins especially specific of the heart conduction system.

Protein spot characterization by computational methods

Some spots were selected for a detailed analysis. The parameters of selected spots (spot quantity, normalized quantity, spot ratio, pI and MW values) are summarized in Table. These parameters were computed during segmentation, quantitative and qualitative analysis of gel images. Essential actions performed during analysis will be explained. Results summarized in Table show that the normalized quantity of 4th and 3rd spots changed most significantly. They changed more than 10 and 7 times, respectively. A significant change was visible in their 3D plots, too (Fig. 3).

After automatic gel segmentation with watershed transformation, manual region editing (splitting or merging) was used. It had to be done because some regions were over-segmented and some of them had more than one spot. Spot detection was performed only in regions marked with red and blue rectangles (Fig. 1 A, B). However, landmark search and selection was performed in full areas (rectangle area plus MW marker). Images were aligned using 89 landmarks. The first stage of landmark search was organized automatically, later the results were processed manually. By manual pairing, some additional landmark

Table. **Results of comparison of two 2DE gel images**

Gel 1 (in red)				Ratio of norm. quantities	Gel 2 (in blue)			
Label	**V_{G1}**	**V_{G1} ($\times 10^{-3}$)**	**Spot center [pI; MW]**	**$\downarrow \equiv \hat{r}_{1/2}$ $\uparrow \equiv \hat{r}_{2/1}$**	**Label**	**V_{G2}**	**V_{G2} ($\times 10^{-3}$)**	**Spot center [pI; MW]**
1r	1897	20.59	[5.1; 20.3]	1.68 ↓	**1.1b**	563.4	6.000	[5.0; 21.1]
					1.2b	546.6	5.822	[5.1; 19.9]
2r	1849	20.07	[4.9; 17.7]	3.24 ↓	**2.1b+ 2.2b**	582.3	6.201	[4.9; 17.7]
3r	808.6	8.778	[4.6; 17.1]	7.36 ↓	**3b**	112.0	1.193	[4.6; 17.1]
4r	494.9	5.372	[4.6; 21.1]	10.5 ↓	**4b**	48.04	0.5116	[4.6; 21.1]
5.1r	96.44	1.047	[6.6; 80.5]	2.68 ↑	**5.1b**	263.7	2.808	[6.6; 80.5]
5.2r	33.10	0.3593	[6.4; 87.5]	2.33 ↑	**5.2b**	78.67	0.8378	[6.4; 87.5]
5.3r	25.48	0.2766	[6.2; 87.5]	1.44 ↑	**5.3b**	37.50	0.3993	[6.2; 87.5]
5.4r	45.64	0.4955	[6.0; 87.5]	1.08 ↓	**5.4b**	43.06	0.4585	[6.0; 87.5]

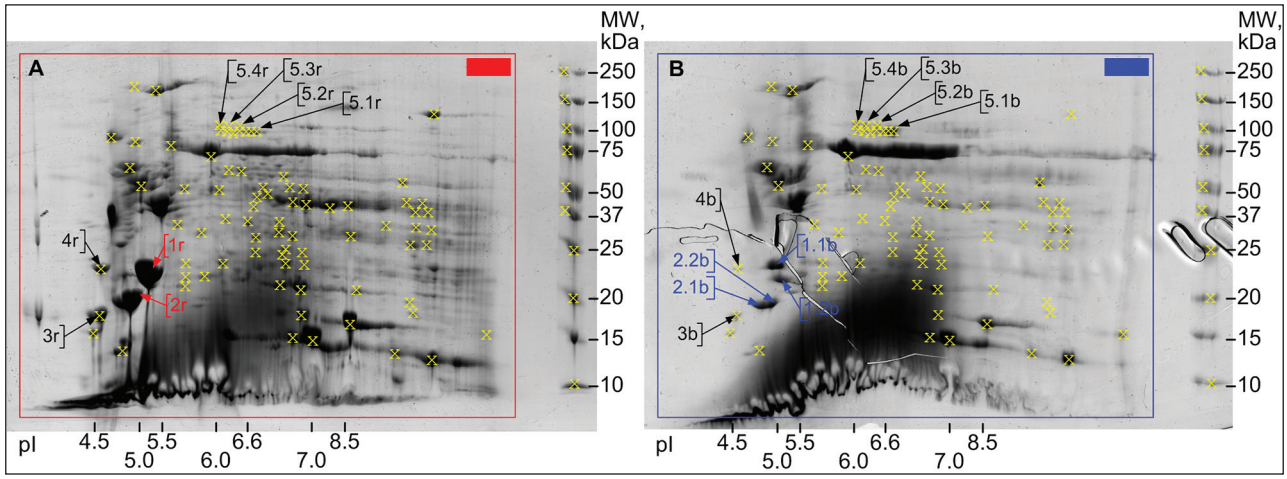

Fig. 1. Two-dimensional electrophoretic maps of proteins isolated from human myocardium and heart conduction system. Total proteins isolated from heart tissues – myocardium (A) and heart conduction system (B) were fractionated by 2-D electrophoresis, and the gels were stained by Coomassie Brilliant Blue G-250 (Fermentas, Lithuania). Molecular weight marker was from Fermentas, Lithuania. Crosses denote selected landmarks used for image registration. The positions of spots selected for a detailed analysis are marked by arrows and numbers in the images. Spot labels ending with in *r* were used only for Gel1 and in *b* for Gel2. Rectangles mark the area used for automatic spot detection. MW markers are left (on the right side of images)

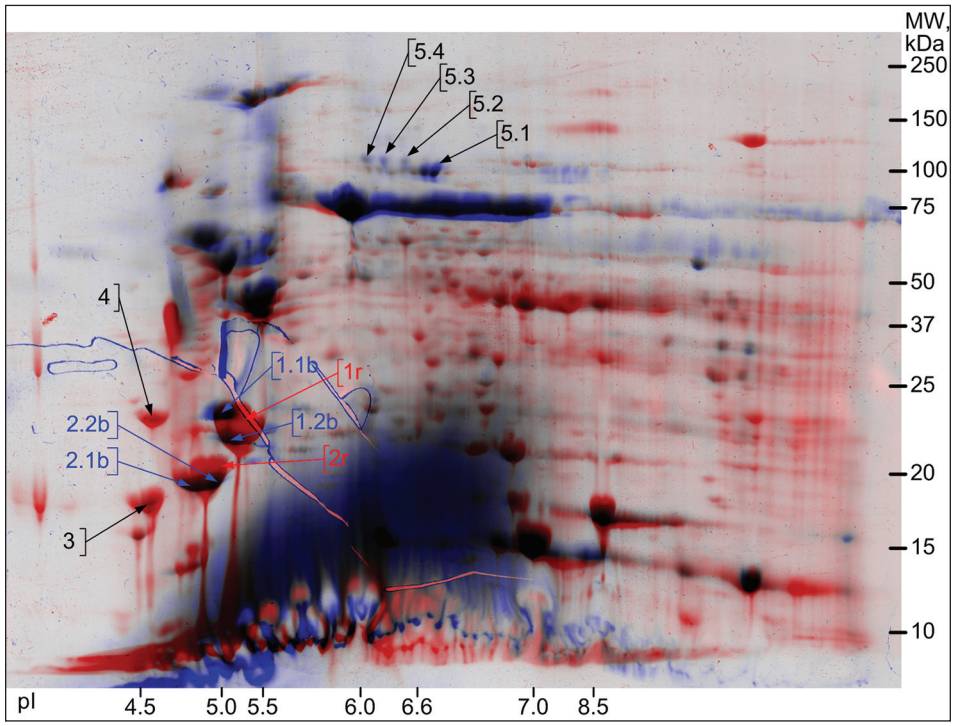

Fig. 2. Gel1 and Gel2 superimposed. Displayed in pseudocolours. Displayed only area of gels marked with rectangle in Fig. 1

were selected in the MW marker area and in some complex regions of gel. The first and the second gel images with selected landmarks are shown in Fig. 1. Figure 2 shows superimposed gel images represented in pseudo-colours and only regions inside rectangles. The pseudo-colour of gel is the same as of the rectangle in Fig. 1. Selected spots for a detailed analysis are labeled. These spots are shown in 3D, too (Fig. 3). The 3rd dimension represents spot intensity.

A standard procedure was used to determine the molecular weight of the polypeptides. The molecular weight of proteins are determined by comparing their mobility with that of several marker proteins (standards) of a known molecular weight. By measuring the migration distance of each protein (standard or unknown) from the top of the resolving gel, the relative mobility (R_f) of each protein was calculated:

$$R_f = \frac{\text{Distance migrated by protein}}{\text{Distance migrated by dye}}.$$

Then a standard curve is generated by plotting the R_f of each standard protein against the log10 of its molecular weight. To estimate the molecular weight of an unknown protein, the standard curve was used to interpolate its log10 molecular weight from its R_f and the antilog ($10^{\log 10(MW)}$) was computed to determine its molecular weight.

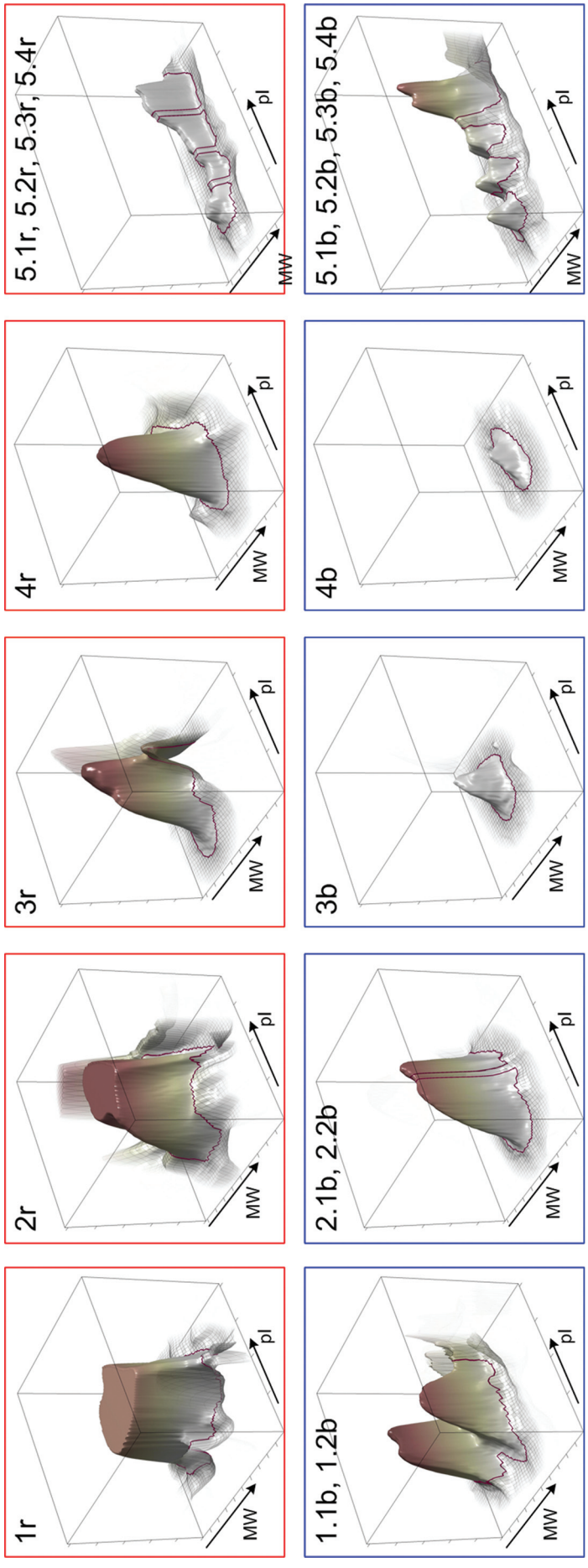

Fig. 3. 3-D plots of selected spots. The 3rd dimension is the intensity of gel image area around a spot

Completion of the described molecular weight determination procedure is a trivial task when the gel is ideal, i. e. free from the geometrical distortions caused by differences in the distances covered by the same molecular mass proteins. In the current images (Fig. 1 A, B), polypeptides on the right side of the gels are noticeably more shifted towards the bottom side. These effects are due to the drawbacks of the electrophoresis technology. A preferred result is polypeptides of the same molecular weight lying in one horizontal line. Practically, technical variations are lowered by running replicate experiments and selecting the best-looking gels. Commercial 2-D electrophoresis image analysis software packages offer the tools for selecting the most appropriate gel as a reference to align all the images to. But there is no guarantee that there will be produced a satisfactory gel to select as a reference. Our approach is to construct the reference gel. Our software has a tool for correcting the horizontal distortions of individual gels. It automatically detects horizontal patterns (polypeptide pathways) in gels and suggests the possible locations for polypeptides of the same molecular weight. The suggested positions can be revised and modified by the user manually. Then, the transformation function is constructed to remap the molecular weights of the observed and marker proteins. Table contains corrected MW values.

Another challenge is to align gels of interest to the pI marker when the pI marker is dried. During drying out, the gel shrinks, and the absolute geometrical positions of spots are moved. This effect yields that the direct manual comparison of gels is very inaccurate. We implemented a tool that helps to bring in a scaling factor which compensates for shrinkage distortions. The image processing tool helped to align gels by their edges and to transfer pI marks. Intermediate pI values were calculated by nonlinear interpolation.

Determination of expression profiles is yet another challenge when comparing gels manually. With the assistance of the software tool, it is possible to compensate for the intensity distortions caused by the varying background, protein detection variations, variations in the amount of a sample. Variations are removed by the use of mathematical spot models, spot quantity normalization and background removal. Background compensation is a required step because it incorrectly influences spot quantity. The spot quantity normalization factor is computed based on the total quantity of all spots, except abundant spots. A new

bell-shaped two-dimensional function was introduced by the authors for spot modeling and quantity parameter estimation. It has been shown to better handle the saturated spots [13]. Computational estimation of protein volume helps to avoid the human factor which influences the subjective gel image analysis. Well known are investigations of human cognitive functions that showed the dependence of object intensity perception on background intensity.

The current gel image analysis was powered by computational tools. Essential data processing tasks were performed by originally developed and implemented algorithms. The image processing software helps to better visualize gel images, highlight significant expression changes, compensate for electrophoresis drawbacks, remove errors caused by human factor, and accelerate research by automating tedious tasks and increasing data reproducibility for future experiments by filing data.

ACKNOWLEDGEMENTS

The research done by D. M. and D. N. was supported through project No. T-08126 (contract No. T-111/08) by the Lithuanian State Science and Studies Foundation.

Received 5 October 2008
Accepted 19 November 2008

References

1. Vivanco F, Darde V, De la Cuesta F, Barderas F. Current Proteomics 2006; 24: 147–70.
2. Venius J, Labeikyte D, Zurauskas E, Strazdaite V, Bagdonas S, Rotomskis R. Biologija 2006; 3: 53–8.
3. Bonaca MP, Morrow DA. Clin Chem 2008; 54: 1424–31.
4. Howes JM, Keen JN, Findlay JB, Carter AM. Diab Vasc Dis Res 2008; 5: 205–12.
5. Matt P, Carrel T, White M et al. J Thorac Cardiovasc Surg 2007; 133: 210–4.
6. Matthiesen R. Proteomics 2007; 7: 2815–32.
7. Raman B, Cheung A, Marten MR. Electrophoresis 2002; 23: 2194–202.
8. Serackis A, Matuzevičius D, Navakauskas D. IC-SPETO 2006; 2: 573–6.
9. Dowsey AW, Dunn MJ, Yang GZ. Proteomics 2003; 3: 1567–96.
10. Matuzevičius D, Navakauskas D. Elektronika ir elektrotechnika 2005; 7: 74–8.
11. Vincent L, Soille P. IEEE Trans Pattern Anal Mach Intell 1991; 13: 583–98.
12. Rogers M, Graham J, Tonge RP. Proteomics 2003; 3: 887–96.
13. Matuzevičius D, Serackis A, Navakauskas D. Elektronika ir elektrotechnika 2007; 1: 63–8.
14. Aittokallio T, Salmi J, Nyman TA, Nevalainen. J Chromatogr A 2005; 815: 25–37.
15. Bookstein FL. IEEE Trans Pattern Anal Mach Intell 1999; 11: 567–85.

Dalius Matuzevičius, Edvardas Žurauskas, Rūta Navakauskienė, Dalius Navakauskas

ŽMOGAUS ŠIRDIES MIOKARDO IR LAIDŽIOSIOS DALIES BALTYMŲ APIBŪDINIMAS SKAITINIAIS METODAIS

Santrauka

Širdies ir kraujagyslių ligos priskiriamos labiausiai paplitusioms ir besibaigiančioms mirtimi išsivysčiusiose šalyse. Žmogaus širdies miokardo ir laidžiosios dalies proteominiai tyrimai, kurie praverstų terapiniams tikslams, dar nėra plačiai atliekami. Mes pritaikėme skaitinius metodus žmogaus širdies miokardo ir laidžiosios dalies baltymams apibūdinti. Šie metodai leido įvertinti baltymų raiškos kaitą miokardo bei laidžiosios dalies proteomo žemėlapiuose bei tiksliai juos charakterizuoti pagal molekulinį svorį bei baltymų pI. Numatomi tolesni baltymų, kurių raiškos lygis kinta miokardo bei širdies laidžiojoje dalyje, identifikavimo tyrimai.